High-pressure study of rhombohedral iron oxide, FeO, at pressures between 41 and 142 GPa

2007 J. Phys.: Condens. Matter 19 036205

(http://iopscience.iop.org/0953-8984/19/3/036205)

INSTITUTE OF PHYSICS PUBLISHING JOURNAL OF PHYSICS: CONDENSED MATTER

J. Phys.: Condens. Matter **19** (2007) 036205 (9pp) doi:10.1088/0953-8984/19/3/036205

High-pressure study of rhombohedral iron oxide, FeO, at pressures between 41 and 142 GPa

S Ono[1,2,5], Y Ohishi[3] and T Kikegawa[4]

[1] Institute for Research on Earth Evolution, Japan Agency for Marine-Earth Science and Technology, 2-15 Natsushima-cho, Yokosuka-shi, Kanagawa 237-0061, Japan
[2] Department of Earth Sciences, University College London, Gower Street, London WC1E 6BT, UK
[3] Japan Synchrotron Radiation Research Institute, 1-1-1, Kouto, Sayo-cho, Sayo-gun, Hyogo 679-5198, Japan
[4] High Energy Acceleration Research Organization, 1-1 Oho, Tsukuba, Ibaraki 305-0801, Japan

E-mail: shigeaki.ono@ucl.ac.uk

Received 25 July 2006, in final form 24 November 2006
Published 5 January 2007
Online at stacks.iop.org/JPhysCM/19/036205

Abstract

In situ observations of the rhombohedral phase in FeO were carried out in a diamond anvil cell high-pressure apparatus using synchrotron x-ray diffraction. The rhombohedral phase remains stable up to at least 142 GPa. However, a discontinuous volume change of 1.6% was observed at about 85 GPa. This volume change was not associated with any change in symmetry. The cell parameter of the *c* axis showed a ∼2.5% reduction at the transition point. In contrast, a small increase (∼0.5%) of the *a* axis was observed. This indicates that the isostructural, first-order phase transition is likely to be due to a change in the magnetic property in FeO at high pressures.

1. Introduction

Iron oxides are of great interest in materials science because they display many diverse electric, magnetic, and optical properties. In addition, the high-pressure study of iron oxides is of interest in earth science because iron oxides are believed to be major constituents of the Earth's interior. The spin transition of iron in iron-bearing magnesium oxide and silicate is now under intense study [1–4] and debate. The ferrous iron oxide wüstite ($Fe_{1-x}O$) is paramagnetic, and crystallizes with a NaCl-type (B1) structure under ambient conditions. As the pressure increases, the NaCl-type structure starts to distort into a rhombohedral structure as observed in a diamond anvil cell (DAC) study using the x-ray diffraction method [5]. A shock compression study reported the existence of a volume reduction of FeO at 70 GPa [6]. Based on observations

[5] Author to whom any correspondence should be addressed. Present address: Department of Earth Sciences, University College London, Gower Street, London WC1E 6BT, UK.

of heated samples using the DAC and synchrotron x-ray diffraction [7, 8], this phase transition is likely to be the result of change from a NaCl-type to a NiAs-type (B8) structures. The phase relation of FeO has also been investigated theoretically [9, 10]. Recently, the magnetic properties of FeO above 100 GPa at room temperature have been investigated by x-ray emission spectroscopy [11], and by Mössbauer spectroscopy [12]. Pasternak *et al* [12] argued that the high-spin to low-spin (HS to LS) transition started at a pressure of 90 GPa. In contrast, Badro *et al* [11] reported that the HS to LS transition was not observed up to a pressure of 143 GPa. This contradiction between experimental studies needs to be resolved. A recent study showed that the HS to LS transition occurred in magnesiowüstite, (Mg, Fe)O, as the pressure increased [2]. In the case of magnesiowüstite, the HS to LS transition was observed in the B1 structure, which was different from rhombohedral FeO.

In this study, we used a laser-heated DAC with the synchrotron x-ray diffraction method. This made it possible to avoid any pressure inhomogeneity in the sample, and to acquire precise x-ray diffraction data on the sample at high pressures. Here we report on the results of *in situ* x-ray observations of the high-pressure phases of FeO. We also determine the phase boundary of rhombohedral FeO without any structural changes, and discuss the magnetic properties of the high-pressure phases of FeO.

2. Experimental procedure

Powdered $Fe_{1-x}O$ with purity 99.9% (Kojundo Chemical Laboratory Corporation, Japan) was used as the starting material. It is known that wüstite, $Fe_{1-x}O$, is a non-stoichiometric compound with a cation deficiency. The composition was established using both x-ray diffraction data and oxygen fugacity methods [13]. Before the experiments, the cell parameter of the starting material was measured, and x was confirmed to be 0.10. High-pressure x-ray diffraction experiments were performed using a laser-heated diamond anvil cell (DAC) apparatus. The sample was ground to a fine powder, and a small pellet with a thickness of less than 10 μm was produced using a hand press. Rhenium gaskets were pre-indented to a thickness of 40 μm and then drilled to give a 50 μm hole. The sample pellet was embedded in sodium chloride (NaCl), and was loaded into a motor-driven DAC with a 60° conical aperture (figure 1). NaCl was used as the pressure-transmitting medium, because it remains a quasi-hydrostatic solid when compared with other harder materials. NaCl was also used as an internal pressure calibrant [14]. The samples were heated with a TEM_{01}-mode Nd:YLF laser or a multimode Nd:YAG laser. The sizes of the heating spots were about 20–30 and 50–100 μm for the YLF and YAG laser, respectively. The sample was heated repeatedly after each pressure change, and x-ray diffraction data were collected at room temperature. The samples were probed by angle-dispersive x-ray diffraction using the synchrotron beam line BL10XU at SPring-8 [15] and BL13A at Photon Factory [16]. The x-ray beam size was collimated to a diameter of 20–30 μm. To adjust the sample position precisely, relative to the x-ray beam position, we monitored the x-ray beam intensity distribution transmitted through the DAC by scanning the DAC stage. The shape of the sample and the gasket hole ware visible in the two-dimensional map of the transmitted x-ray intensity. According to this x-ray map, we could set the sample precisely relative to the x-ray beam position. Angle-dispersive x-ray diffraction patterns were obtained on an imaging plate (Rigaku, Japan). The distance between the sample and the detectors was measured using CeO_2 as a standard. The observed intensities on the imaging plates were integrated as a function of 2θ to give conventional, one-dimensional diffraction profiles. The typical uncertainty of the angular resolution of the integrated diffraction pattern was about 0.01°. The diffraction peak positions were determined by a peak-fitting program using a Gaussian function, and the unit cell parameters and volumes

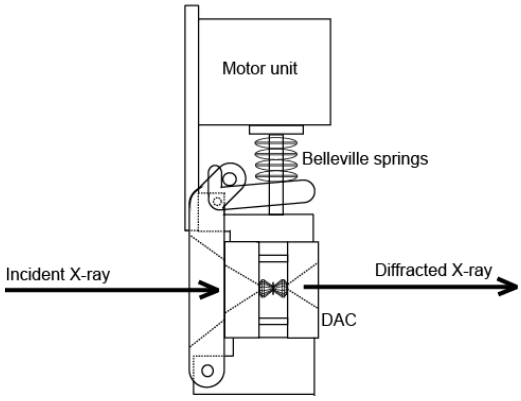

Figure 1. Motor-driven diamond anvil cell assembly. The diamond anvil cell was mounted in a lever arm, that was driven by a spring screw system. The screw was rotated by a stepping motor unit in order to change the pressure. The Belleville spring stabilizes the pressure generation.

of the sample were calculated using a least-squares fit of each diffraction peak position. The pressure was determined from the measured unit volume of the NaCl unit cell using the equation of state (EOS) for NaCl by Ono *et al* [14].

3. Results

In the DAC experiments, x-ray diffraction data were acquired at each pressure increment following the laser heating. After the desired pressure was achieved, the sample was heated to relax the differential stress, and to overcome potential kinetic effects on the phase transition. Heating durations were between 5 and 10 min. Subsequently, the laser power was decreased gradually to avoid accumulation of differential stress in the sample during the temperature quench. After heating, the diffraction peaks were observed to sharpen due to the relaxation of differential stress. Typical diffraction patterns are reproduced in figure 2. Most diffraction peaks belonged to the sample. Unexpected extra small peaks sometimes appeared, such as at the 10° position in figure 2. Exposure times were typically between 10 and 20 min. The pressure was calculated from the EOS of NaCl using at least four diffraction lines (100, 110, 200, and 211). In addition to the peaks arising from CsCl-type (B2-type) NaCl, other peaks were observed, indicating that the initial sample material had transformed into a high-pressure phase. These peaks belonged to the rhombohedral cell, and were identified as due to the high-pressure phase of FeO, which distorted from cubic symmetry. Although the experiment was performed up to a pressure of 142 GPa, no further transition was observed in this study.

In the first set of LHDAC experiments, the pressure was increased directly to ∼45 GPa, at room temperature. After the desired pressure was achieved, the sample was heated to ∼1500 K to relax the differential stress. After heating, the sample pressure decreased to 41 GPa, due to stress relaxation in the sample chamber. Moreover, the sample was compressed gradually to 61 GPa. The volume of rhombohedral FeO decreased continuously as the pressure increased (figure 3).

In the second run, the initial pressure was increased to ∼60 GPa, and an x-ray diffraction pattern of the rhombohedral FeO was recorded at each pressure increment as the pressure increased gradually up to 97 GPa. No change in the x-ray diffraction pattern was observed. This indicated that there was no structural phase transition in this pressure range. Table 1 shows the fitted results of the x-ray diffraction peaks of rhombohedral FeO at 79 and 90 GPa.

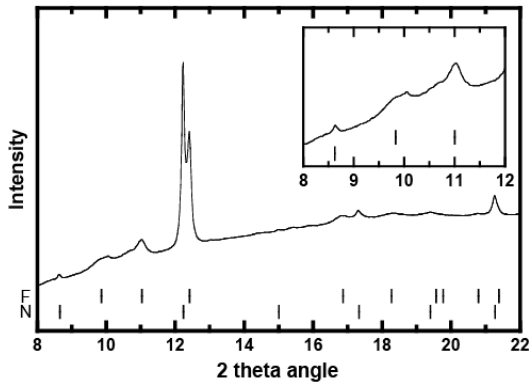

Figure 2. An example of observed x-ray diffraction patterns of the sample. Data were acquired at 97 GPa and 300 K after heating. Vertical bars indicate the calculated positions of the diffraction lines of each phase. Rhombohedral FeO, $a = 2.609$ Å and $c = 7.237$ Å; B2-type NaCl, $a = 2.748$ Å. Abbreviations used are as follows: F, rhombohedral FeO; N, B2-type NaCl.

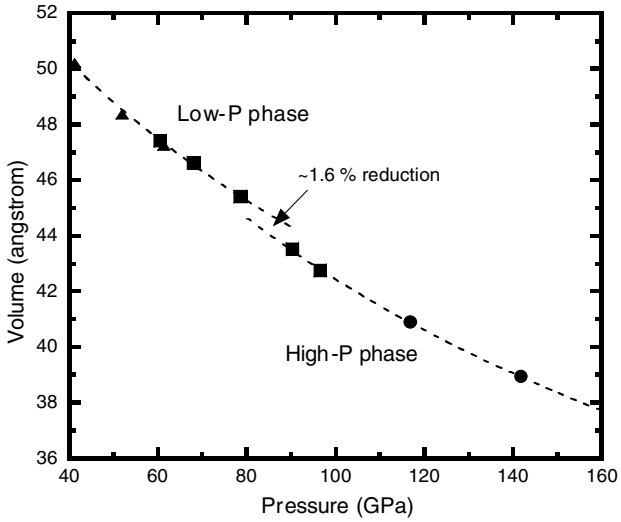

Figure 3. Pressure–volume data for rhombohedral FeO at 300 K. Triangles, run #1; squares, run #2; circles, run #3 (see table 2). Dashed lines are the Birch–Murnaghan equation fits for volumes of each phase ($B_0' = 4$). The transition pressure was ∼85 GPa. Errors are smaller than the symbols.

We could not confirm any differences in the fitted results for data taken at 79 and 90 GPa. However, a significant discontinuity in the volume change, of ∼1.6%, was observed (figure 3). In the third run, the sample was investigated from 117 to 142 GPa. No volume discontinuity or structural change was observed over the higher pressure range.

The effect of pressure on the unit cell parameters and the volume of rhombohedral FeO are shown by the data listed in table 2. The P–V data of each low- and high-pressure phase were fitted to the third-order Birch–Murnaghan equation of state to determine the elastic parameters,

$$P = \tfrac{3}{2}B_0(x^{-7} - x^{-5})[1 + \tfrac{3}{4}(B_0' - 4)(x^{-2} - 1)],$$

where $x = (\frac{V}{V_0})^{\frac{1}{3}}$; and V_0, B_0, and B_0' are, respectively, the volume, isothermal bulk modulus, and first pressure derivative of the isothermal bulk modulus. At first we used data for the low-

Table 1. Observed and calculated x-ray diffraction peaks of rhombohedral FeO at 79 and 90 GPa. (Calculated d-spacings are based on hexagonal unit cell dimensions ($a = 2.635(1)$ Å, $c = 7.551(4)$ Å at 78.6 GPa; $a = 2.618(1)$ Å, $c = 7.334(6)$ Å at 90.3 GPa).)

	78.6 GPa			90.3 GPa		
HKL	d_{obs} (Å)	d_{cal} (Å)	d_{obs}–d_{cal}	d_{obs} (Å)	d_{cal} (Å)	d_{obs}–d_{cal}
101	2.183	2.185	−0.002	2.168	2.166	0.002
102	1.953	1.953	0.000	1.930	1.928	0.002
104	1.455	1.455	0.000	1.425	1.426	−0.001
110	1.318	1.318	0.000	1.309	1.309	0.000

Table 2. Lattice parameters and volumes of rhombohedral FeO for pressures up to 142 GPa at 300 K. (Numbers in parentheses represent the error in the lattice parameter and volume of rhombohedral FeO based on a hexagonal unit cell. Pressures were determined from the observed unit cell volume of B2-type NaCl using the equation of state for NaCl [14]. The wavelength of the monochromatic incident x-ray beam: run #1, $\lambda = 0.4276$ Å at Photon Factory; runs #2 and #3, $\lambda = 0.4139$ Å at SPring-8. The wavelength of x-ray was determined using the CeO_2 standard.)

P (GPa)	a (Å)	c (Å)	Volume (Å^3)	c/a
		Run #1		
41.3(2)	2.754(2)	7.640(14)	50.18(11)	2.774(7)
51.9(2)	2.707(1)	7.625(3)	48.39(3)	2.817(2)
61.4(1)	2.677(1)	7.611(6)	47.24(5)	2.843(3)
		Run #2		
60.5(1)	2.687(2)	7.585(11)	47.43(10)	2.823(6)
68.1(3)	2.664(1)	7.585(4)	46.62(3)	2.847(2)
78.6(2)	2.635(1)	7.551(4)	45.40(3)	2.865(2)
90.3(1)	2.618(1)	7.334(6)	43.53(4)	2.802(3)
96.6(1)	2.599(1)	7.307(7)	42.74(6)	2.811(4)
		Run #3		
116.9(3)	2.561(1)	7.200(4)	40.90(4)	2.811(3)
141.8(4)	2.513(2)	7.120(6)	38.94(6)	2.833(4)

Table 3. Comparison of bulk modulus between high-spin and low-spin phases. (Numbers in parentheses represent the fitting error of the bulk modulus and volume of rhombohedral FeO.)

	B (GPa)	B'	V (Å^3)
High-spin state at 0 GPa	168(11)	4[a]	59.56(61)
at 85 GPa	490(11)	4[a]	44.83(7)
Low-spin state at 85 GPa	355(6)	4[a]	44.14(5)

[a] B' was set to 4.

pressure phase at pressures lower than 85 GPa to fit the volume to the equation of state. When the value of B'_0 was set to $B'_0 = 4$, the isothermal bulk modulus and the volume at 0 GPa were determined to be $B_0 = 168(11)$ GPa, and $V_0 = 59.56(61)$ Å^3, respectively (table 3). The volume data for the high-pressure phase at pressures higher than 85 GPa were also fitted to the Birch–Murnaghan equation of state. When the value of B'_0 was set to $B'_0 = 4$, the isothermal bulk modulus and the volume at 85 GPa were determined to be $B_{85} = 355(6)$ GPa and $V_{85} = 44.14(5)$ Å^3, respectively.

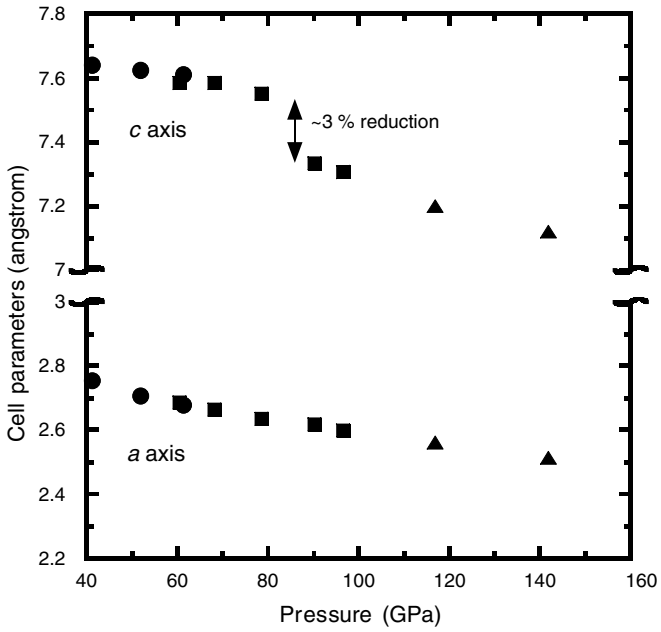

Figure 4. Unit cell parameters of rhombohedral FeO as a function of pressure. Circles, run #1; squares, run #2; triangles, run #3 (see table 2). Errors are smaller than the symbols.

Figure 4 shows the change in cell parameters of rhombohedral FeO. The volume discontinuity was observed between 79 and 90 GPa. A small increase in the a axis was identified. In contrast, an obvious reduction was confirmed in the c axis between 79 and 90 GPa. The length reduction in the c axis was $\sim$2.5%. This indicated that the discontinuous volume change was due to the drastic change in the c axis.

The c/a ratio of rhombohedral FeO as a function of pressure is plotted in figure 5. The c/a ratio increased as the pressure increased. A significant difference of the c/a slope can be observed between low and high pressures. The P–c/a data were fitted to a linear equation to determine the slope:

$$c/a = 2.685 + 0.002\,37P \ (<85 \text{ GPa})$$
$$c/a = 2.755 + 0.000\,53P \ (P>85 \text{ GPa}),$$

where P is the pressure (GPa). The discontinuity of the c/a ratio was confirmed at 85 GPa. Although the c/a ratio increased gradually up to $\sim$80 GPa, an abrupt decrease occurred at a pressure of $\sim$85 GPa, and then the ratio increased again. The slope at higher pressures became smaller than that at lower pressures.

4. Discussion

The lattice distortion can be described as the c/a ratio. When c/a is equal to $\sqrt{6}$, there is no rhombohedral distortion (an exact cubic cell). According to our experimental data, the distortion increased as the pressure increased. The increase in the c/a ratio means that the cell is elongated along the [111] direction of the cubic cell. This observation is in good agreement with the theoretical prediction [10].

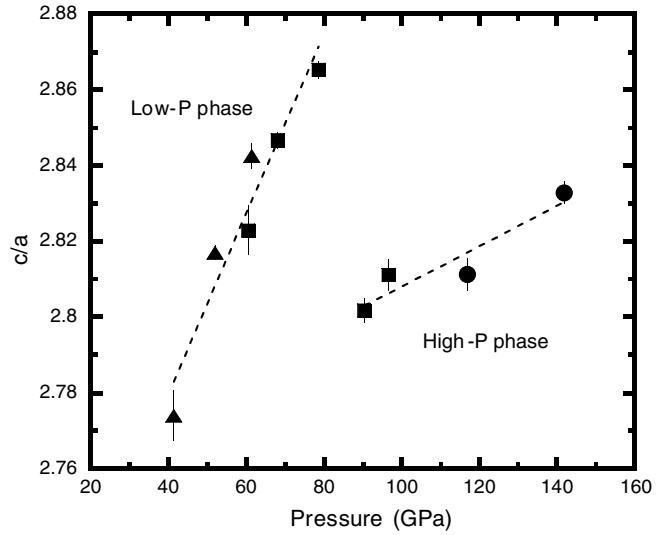

Figure 5. The c/a ratio of the rhombohedral cell in FeO as a function of pressure. Triangles, run #1; squares, run #2; circles, run #3 (see table 2). Dashed lines are linear fits for the c/a values of each phase. Vertical bars denote errors.

Although a crystallographic transition of rhombohedral FeO was not observed at the high pressures investigated in this study, the interesting features of the cell parameters and the volume reduction at ∼85 GPa were confirmed. A possible explanation for these features is that a pressure-induced magnetic spin transition in iron occurs in rhombohedral FeO. It is known that the HS to LS transition of iron occurs in some iron-bearing materials [2, 17, 18]. When the HS to LS transition occurs, the effective ionic radius of iron decreases. This decrease in the ionic radius can induce a discontinuous volume reduction without any crystallographic phase transition. In the case of the (Mg, Fe)O study, volume reductions due to the HS to LS transition were observed at high pressures [2]. The discrepancy between the previous (Mg, Fe)O study and our FeO study was confirmed. A continuous volume reduction was observed in the previous (Mg, Fe)O study. In contrast, our FeO study showed that the volume change was discontinuous. This discrepancy is likely to be due to the pressure inhomogeneity in the sample: in the previous (Mg, Fe)O study the sample was compressed at room temperature. It is known that significant stress is accumulated during compression in DAC experiments. As the experimental results might be ambiguous because of this accumulated stress, we used laser heating to release the stress in the sample. Therefore, a sharp change in volume could be observed in our study. In the case of a two-component system (MgO and FeO), the coexisting state can appear at intermediate pressures.

Pasternak *et al* [12], using Mössbauer spectroscopy, suggested that the HS to LS transition occurred in the pressure range of 90–140 GPa at $T \leqslant 300$ K. In contrast, x-ray emission spectroscopy showed that the HS state in FeO remained stable up to 143 GPa at room temperature [11]. This apparent contradiction can be resolved by our experimental results. The sharp volume discontinuity in FeO could be observed for the first time by using annealing to release the pressure inhomogeneity in the sample. Using x-ray emission spectroscopy it is difficult to identify the coexisting HS and LS states due to the pressure inhomogeneity, because the identification of the spin state is based solely on the Kβ' peak emission. In the case of Mössbauer spectroscopy studies, the coexisting state could be observed clearly, because

the spectra of the coexisting state were quite different from those of the single state. The Mössbauer spectroscopy data showed that the coexisting state started at 90 GPa, which is in agreement with the HS to LS transition pressure (∼85 GPa) observed in our x-ray diffraction study. Therefore, it is likely that pressure inhomogeneity during room-temperature compression may have caused the misleading interpretations in previous studies. As it is difficult to prepare stoichiometric FeO, the chemical compositions of iron oxide used in previous studies were $Fe_{0.92}O$–$Fe_{0.94}O$. The influence of the chemical composition on the spin transition may not be negligible. Therefore, it is necessary to investigate the effect of chemical composition in a future study.

In the case of Mössbauer spectroscopy [12], this HS to LS transition seemed to be a second-order transition, because the coexisting state was observed. However, we were able to observe the discontinuous changes in volume, cell parameter, and the c/a ratio. These indicated that this HS to LS transition was a first-order transition. Therefore using a stress-free sample at high pressures, both Mössbauer spectroscopy and x-ray emission spectroscopy can confirm the first-order transition in FeO associated with the spin transition.

Recent studies using high-resolution Kβ x-ray emission spectroscopy showed that there is a possibility that the spin transition of iron-bearing minerals, perovskite and ferropericlase, may occur in the Earth's lower mantle [1–4]. As both minerals are major constitutes of the lower mantle [19], it is important to know their behaviour at high pressures for the earth science community. However, the spin transition of perovskite is a disputable issue, because there is a significant discrepancy among some high-pressure experiment groups. Our study showed that pressure inhomogeneity in the high-pressure cell caused the misleading conclusion. Therefore, the pressure needed for the spin transition of perovskite could be overestimated in previous studies using the emission spectroscopy method.

Acknowledgments

The synchrotron radiation experiments were performed at SPring-8, JASRI (Proposal No. 2006A1412) and at the Photon Factory, KEK (Proposal Nos 2003G187 and 2005G122). This work was partially supported by a Grant-in-Aid for Scientific Research from the Ministry of Education, Culture, Sport, Science and Technology, Japan.

References

[1] Badro J, Rueff J P, Vankó G, Monaco G, Fiquet G and Guyot F 2004 *Science* **305** 383
[2] Lin J F, Struzhkin V V, Jacobsen S D, Hu M Y, Chow P, Hung J, Liu H, Mao H K and Hemley R J 2005 *Nature* **436** 377
[3] Jackson J M, Sturhahn W, Shen G, Zhao J, Hu M Y, Errandonea D, Bass J D and Fei Y 2005 *Am. Mineral.* **90** 199
[4] Zhang F and Oganov A R 2006 *Earth Planet. Sci. Lett.* **249** 436
[5] Zou G, Mao H K, Bell P M and Virgo D 1980 *Yearbook Carnegie Inst. Washington* **79** 374
[6] Jeanloz R and Ahrens T J 1980 *Geophys. J. R. Astron. Soc.* **62** 505
[7] Fei Y and Mao H K 1994 *Science* **266** 1668
[8] Kondo T, Ohtani E, Hirao N, Yagi T and Kikegawa T 2004 *Phys. Earth Planet. Inter.* **143/144** 201
[9] Mazin II, Fei Y, Downs R and Cohen R 1998 *Am. Mineral.* **83** 451
[10] Fang Z, Solovyev I V, Sawada H and Terakura K 1999 *Phys. Rev.* B **59** 762
[11] Badro J, Struzhkin V V, Shu J, Hemley R J, Mao H K, Kao C C, Rueff J P and Shen G 1999 *Phys. Rev. Lett.* **83** 4101
[12] Pasternak M P, Taylor R D, Jeanloz R, Li X, Nguyen J H and McCammon C A 1997 *Phys. Rev. Lett.* **79** 5046
[13] McCammon C A and Liu L 1984 *Phys. Chem. Minerals* **10** 106
[14] Ono S, Kikegawa T and Ohishi Y 2006 *Solid State Commun.* **137** 517

[15] Ono S, Funakoshi K, Ohishi Y and Takahashi E 2005 *J. Phys.: Condens. Matter* **17** 269
[16] Ono S, Funakoshi K, Nozawa A and Kikegawa T 2005 *J. Appl. Phys.* **97** 073523
[17] Badro J, Fiquet G, Struzhkin V V, Somayazulu M, Mao H K, Shen G and Bihan T L 2002 *Phys. Rev. Lett.* **89** 205504
[18] Li J, Struzhkin V V, Mao H K, Shu J, Hemley R J, Fei Y, Mysen B, Dera P, Prakapenka V and Shen G 2004 *Proc. Natl Acad. Sci.* **101** 14027
[19] Ono S and Oganov A R 2005 *Earth Planet. Sci. Lett.* **236** 914